CEC/ICMC 2015
June 29-July 4 2015
JW Marriott Starr Pass Resort & Spa,
Tucson, Arizona

R&D status of highly efficient Stirling-type cryocooler for superconducting drive motor

J Watanabe, T Nakamura, S Iriyama,
T Ogasa, N Amemiya(*Kyoto University, Japan*);
Y Ohashi(*AISHIN SEIKI Co.,Ltd , Japan*)

京都大学
KYOTO UNIVERSITY

Outline

1. Background and objective
2. Specifications of developed compressor
3. Analytical and experimental method
4. Results and discussion
5. Development and test of pulse-tube cryocooler
6. Conclusion

1. Background and objective

Target ;

Drive motor for the next generation electric vehicle

High Temperature Superconductor Induction/Synchronous Machine

HTS-ISM

Advantages

- High efficiency thanks to synchronous rotation
- High torque density
- Stable Rotation

Direct-drive without transmission gears

京都大学 KYOTO UNIVERSITY

1. Background and objective

Necessary functions of the cryocooler for HTS-ISM system

- High efficiency
- Light weight
- Robustness against vibration

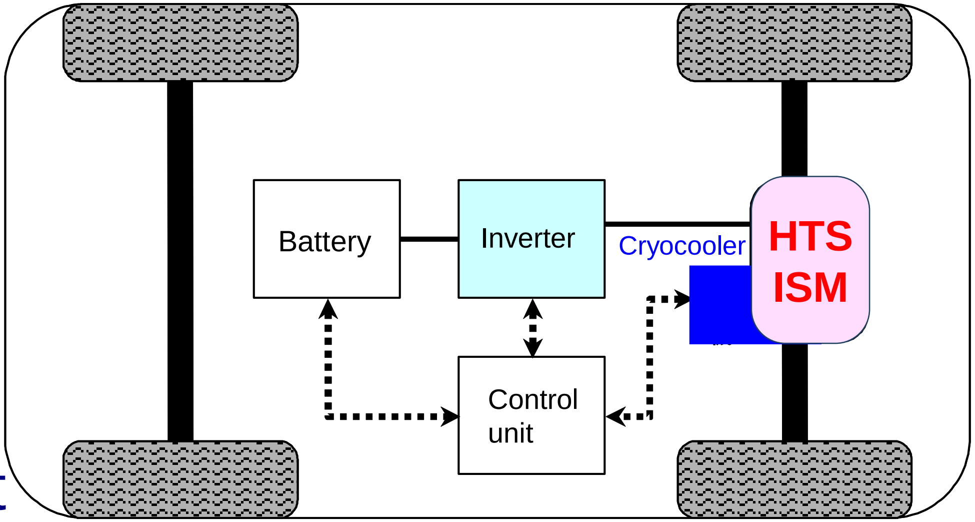

Fig.1 Schematic diagram of direct-derived power train system

Development of highly efficient Stirling-type cryocooler

Development of linear actuator-type compressor

Moving magnet type linear actuator

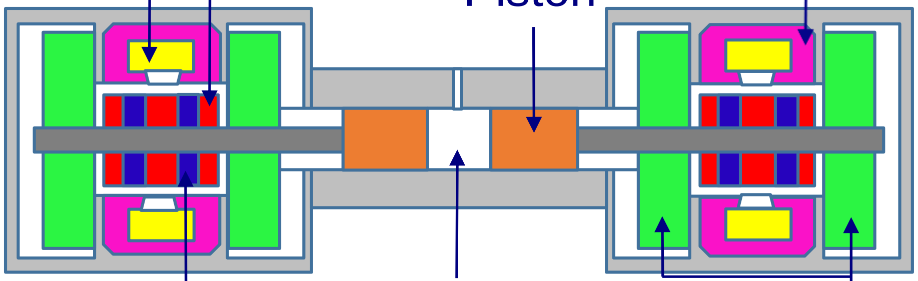

Fig.2 Schematic diagram of compressor

Table1 Specifications of compressor

Input	3000 W
Coil Wire diameter	1.6 mm
Turn number of coil	210
DC resistance	0.6 Ω
Rated stroke length	±10 mm
Piston diameter	40 mm

3. Analytical and experimental method

Finite element method analysis model

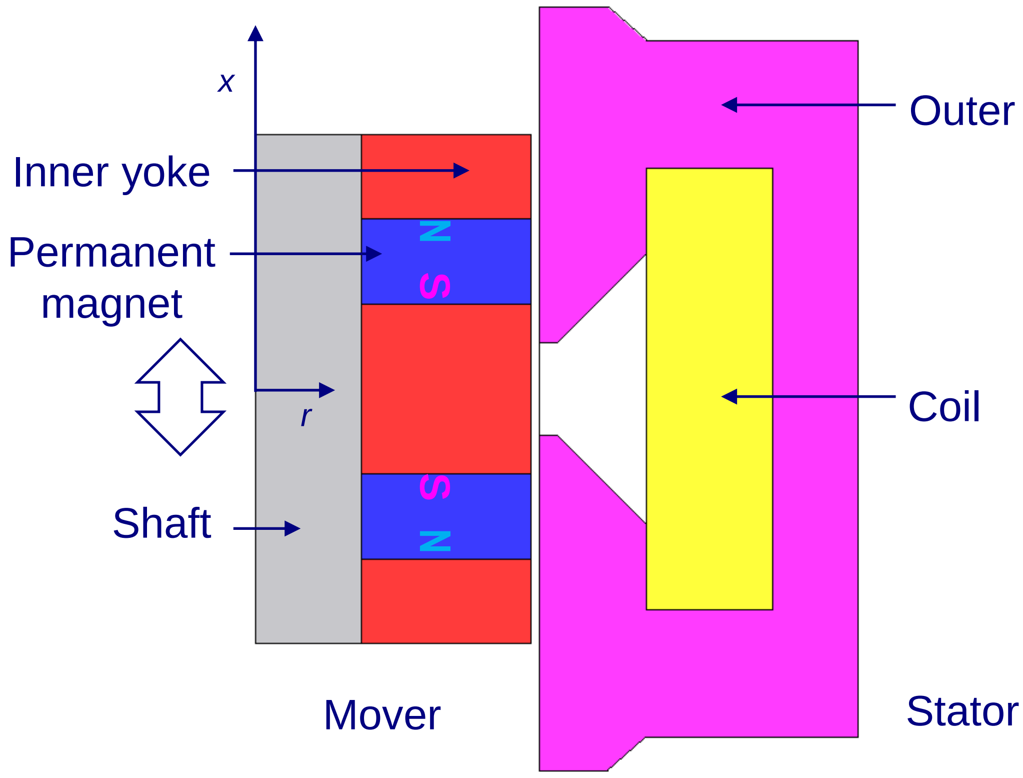

Analysis by commercial software(JMAG-Designer®)

(Analysis conditions)
External circuit :
Single-phase current source
Mover motion :
Forced displacement

Fig.3 Axisymmetric analysis model of the linear actuator

3. Analytical and experimental method

Electromagnetic field analysis code coupled with kinetic equation

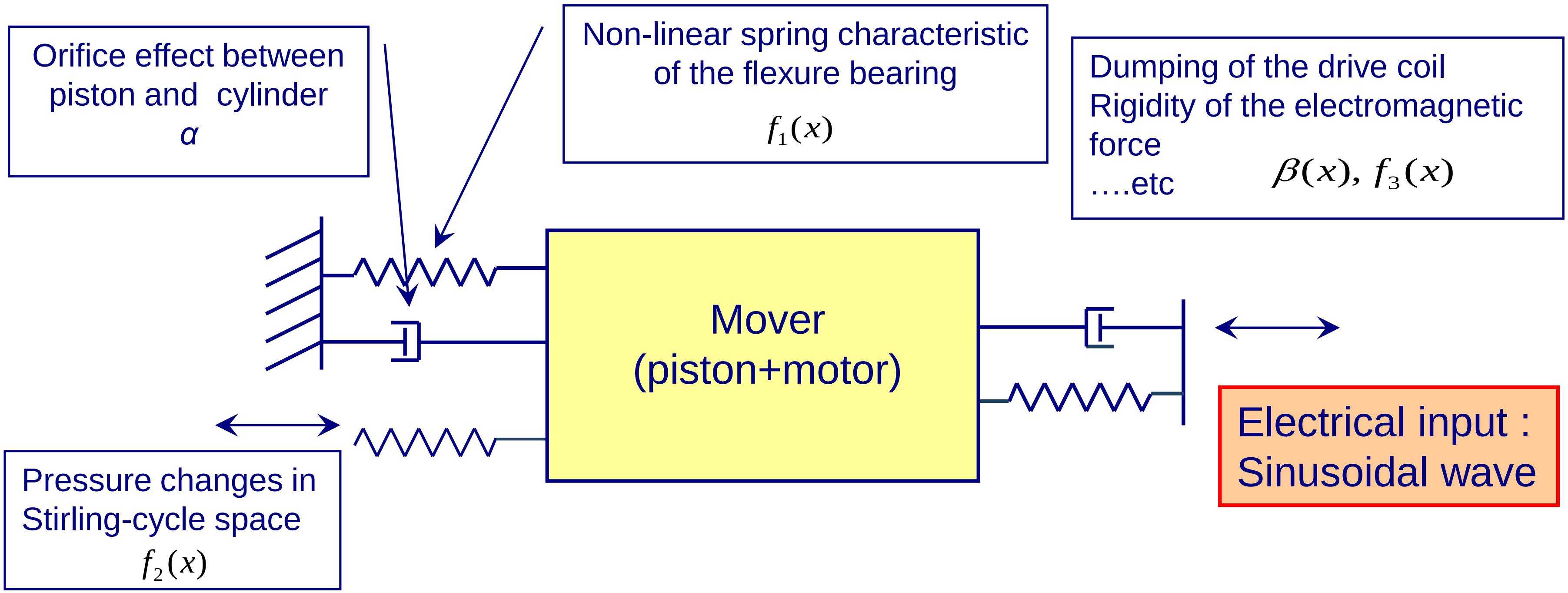

$$m\frac{d^2x}{dt^2}+(\alpha+\beta(x))\frac{dx}{dt}+(f_1(x)+f_2(x)+f_3(x))x=\sum_n a_n \sin n\omega t$$

Fig.4 Analysis model of the actuator

3. Analytical and experimental method

Experimental method under no-load condition

Fig.6 Photograph of compressor assembly

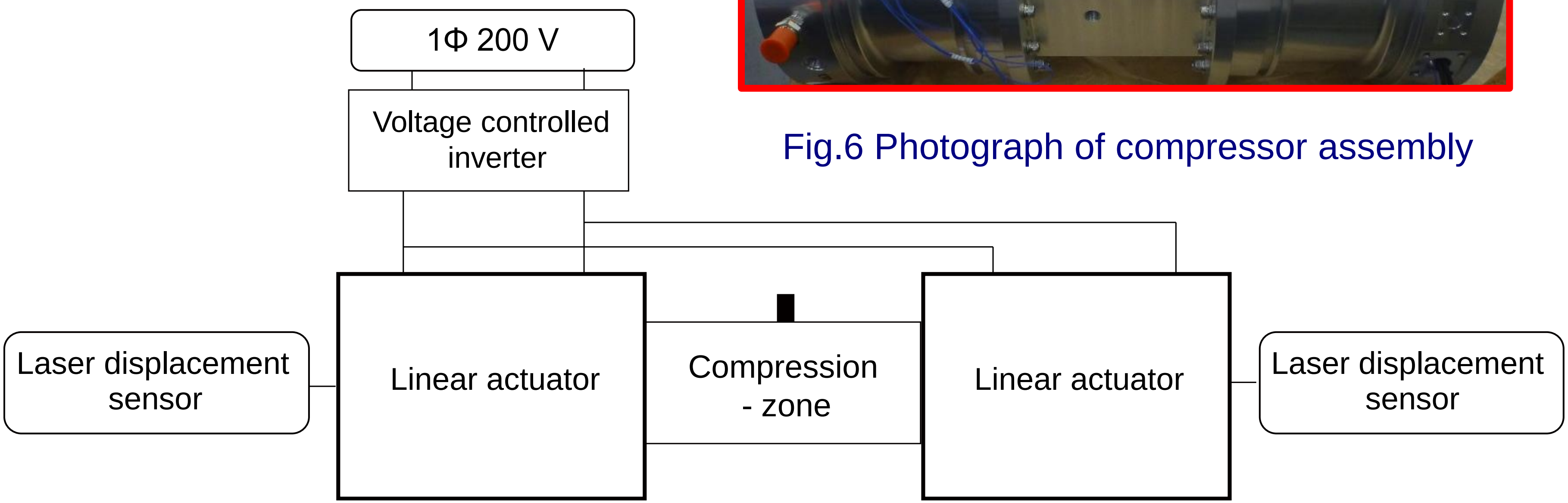

Fig.5 Schematic diagram of experiment under no-load condition

3. Analytical and experimental method

Load test of the compressor with He gas

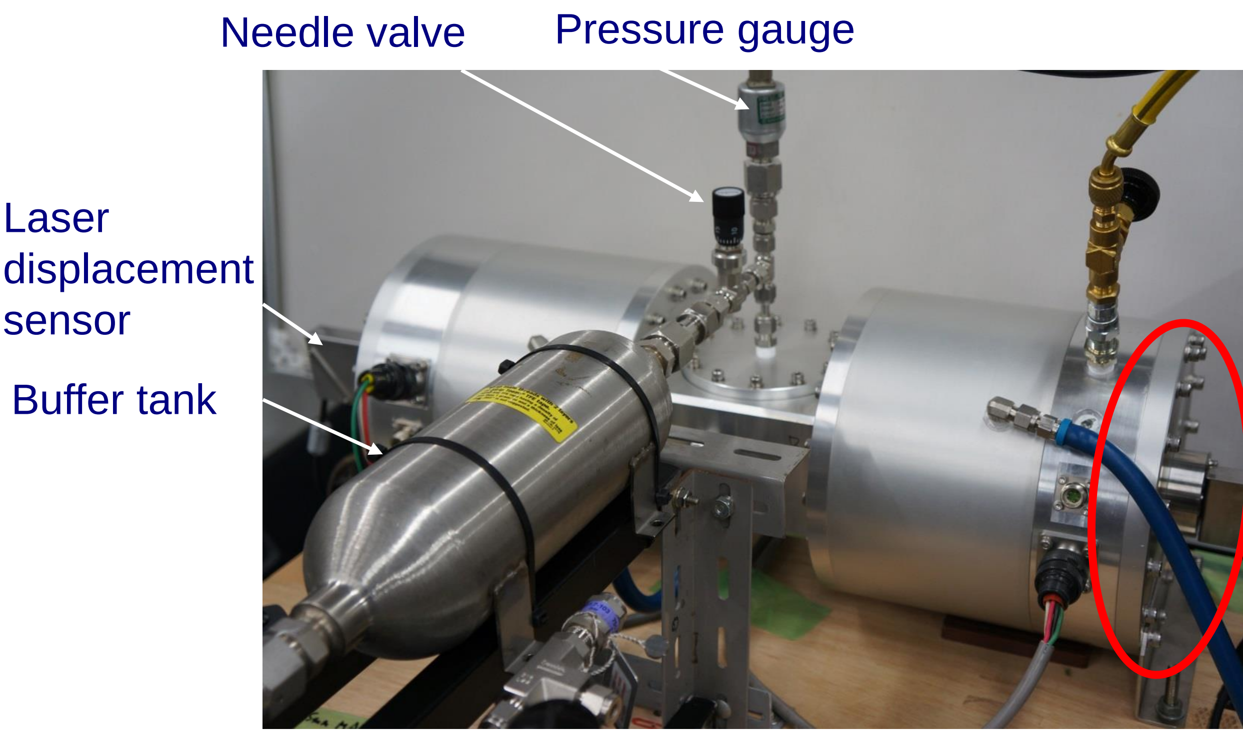

Fig.7 Photograph of experimental system under load condition

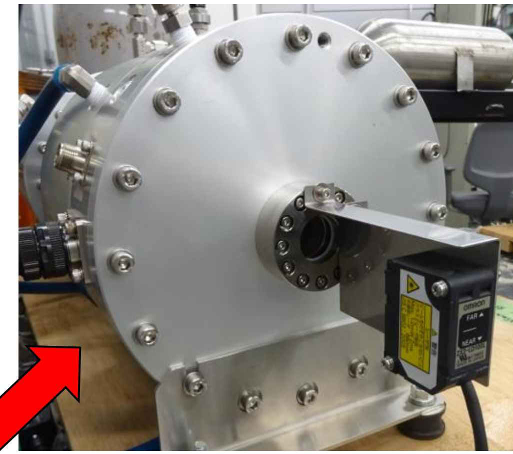

Fig.8 Laser displacement sensor

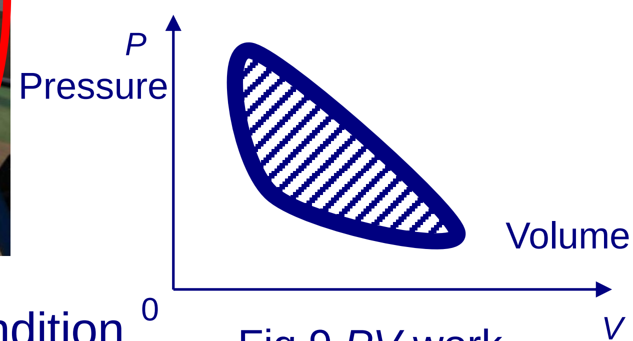

Fig.9 *PV* work

4. Results and discussion

Drive frequency 42 Hz, Displacement 5 mm, 10 mm (experimental results)

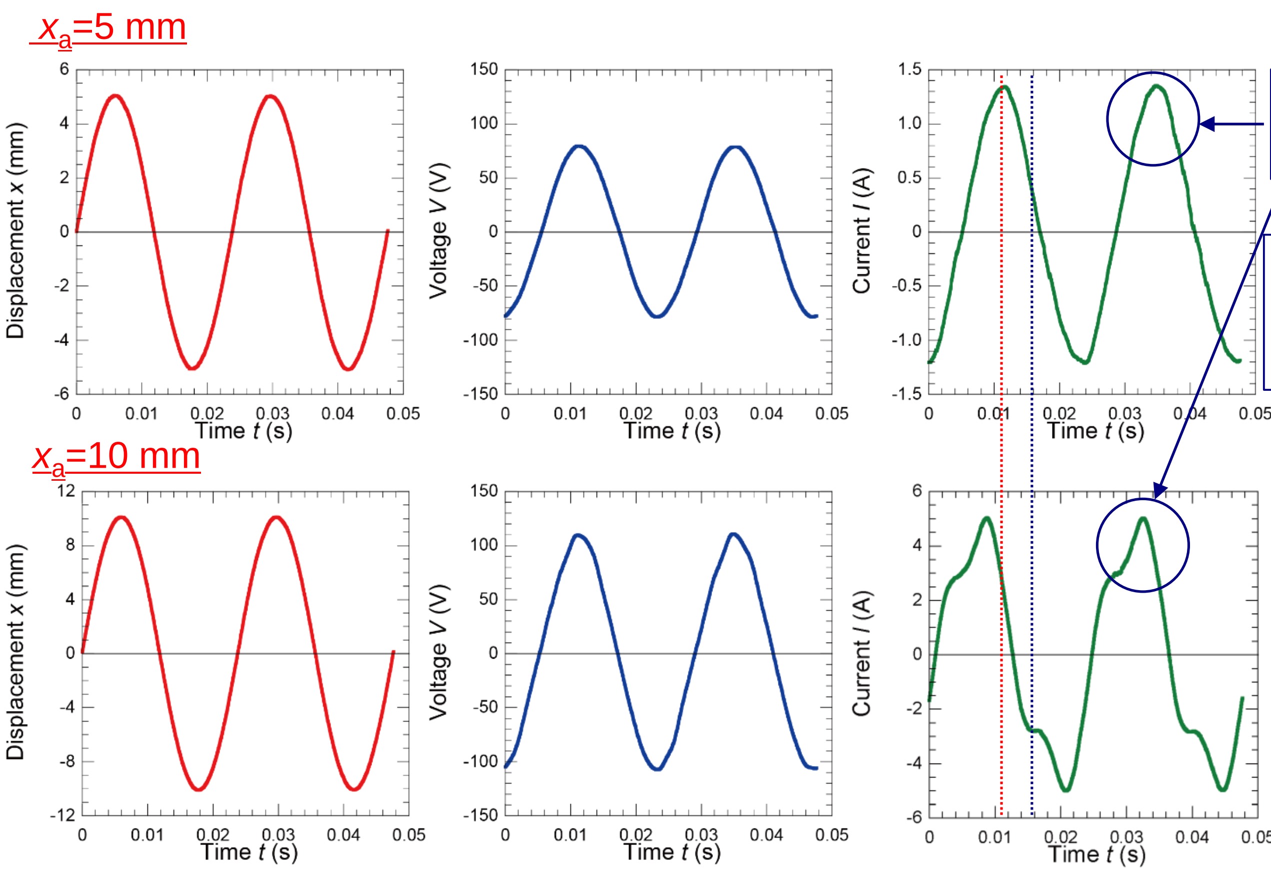

(a) Displacement (b) Voltage (c) Current

Fig.10 Experimental results under no-load condition

In case of x_a=10 mm, the current waveform was distorted.

The power factor was decreased because phase of the current waveform lagged.

Detailed examination by analysis

4. Results and discussion

The FFT analysis of the current waveform
→Third harmonic component was highly included

Current waveform obtained by superimposing the third harmonic

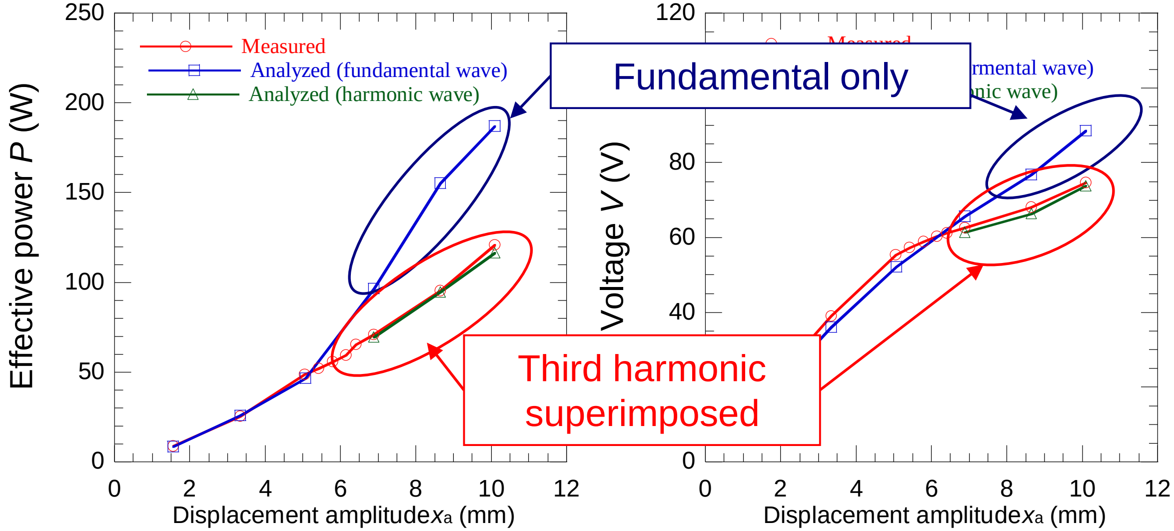

(a) Effective power

(b) Voltage

Fig.12 Experimental and analysis results under no-load condition

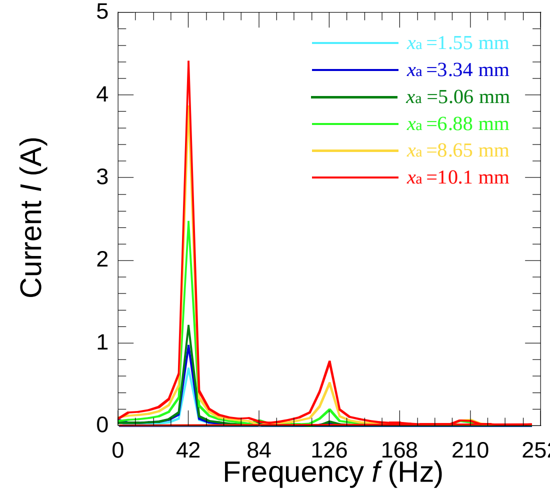

Fig.11 Power spectrum of current waveform

Agreement between experimental and analysis results

Reason for the current waveform distortion

4. Results and discussion

The counter-electromotive force in the case of forced displacement (analysis results)

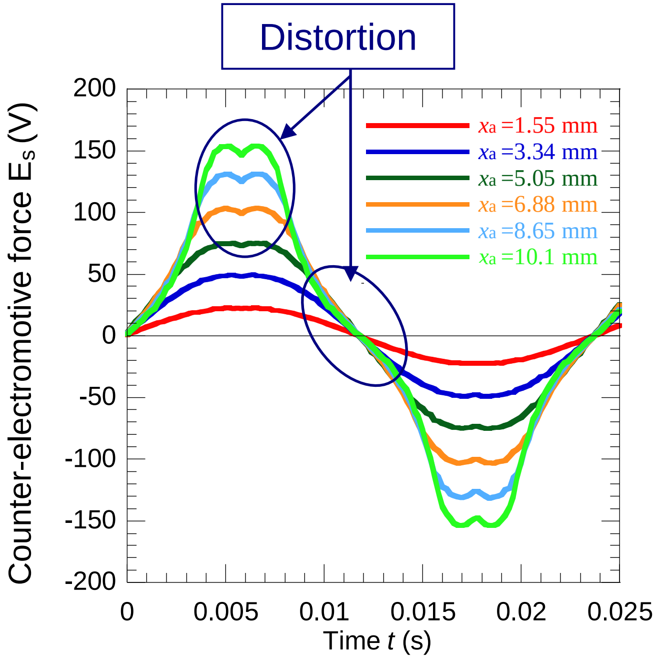

(a) Waveform

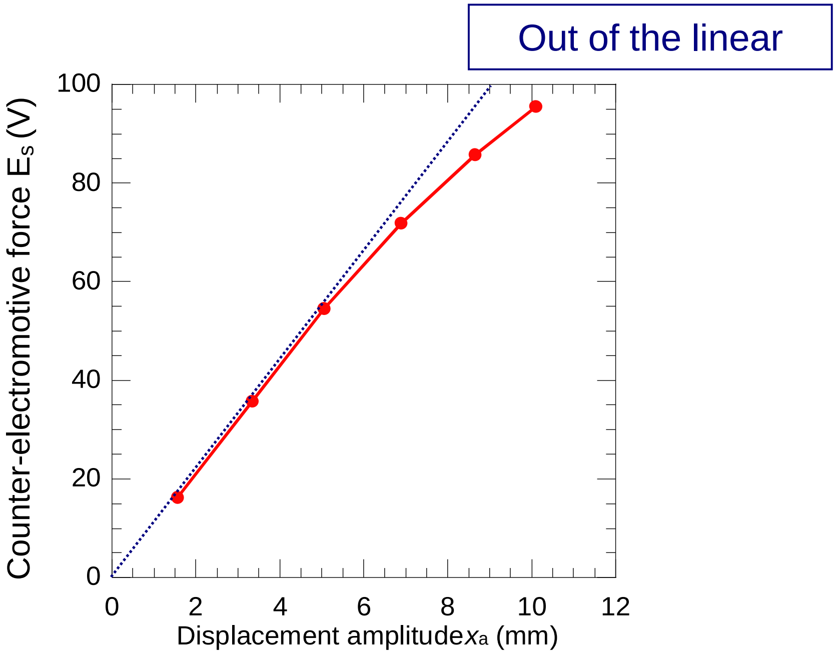

(b) Effective value

Fig.13 Analysis results of counter-electromotive force

→ Distortion of the waveform caused by nonlinear B-H curve

Output characteristics (analysis results)

Displacement 10.0 mm, Frequency 58 Hz, Current - displacement phase difference 90 °

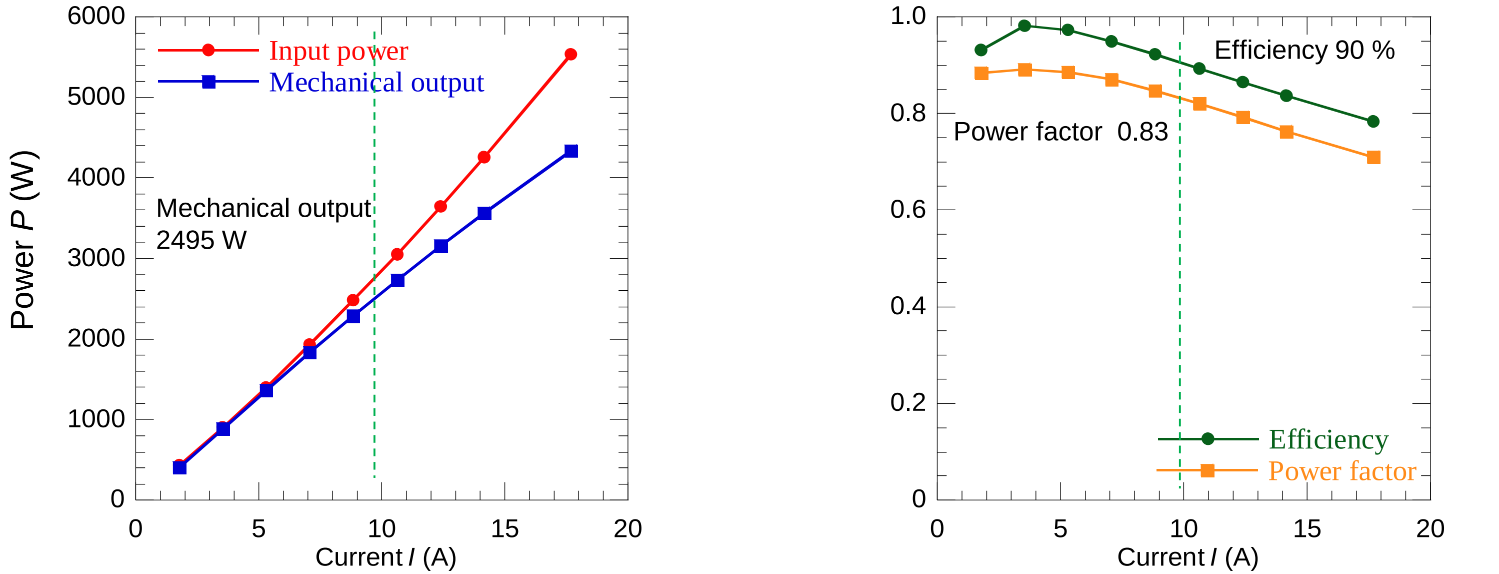

Fig.14 Output characteristics (analysis results)

→ Possibility of high efficiency and power factor

4. Results and discussion

Frequency 59 Hz Pressure 2.5 MPa Input 200 V

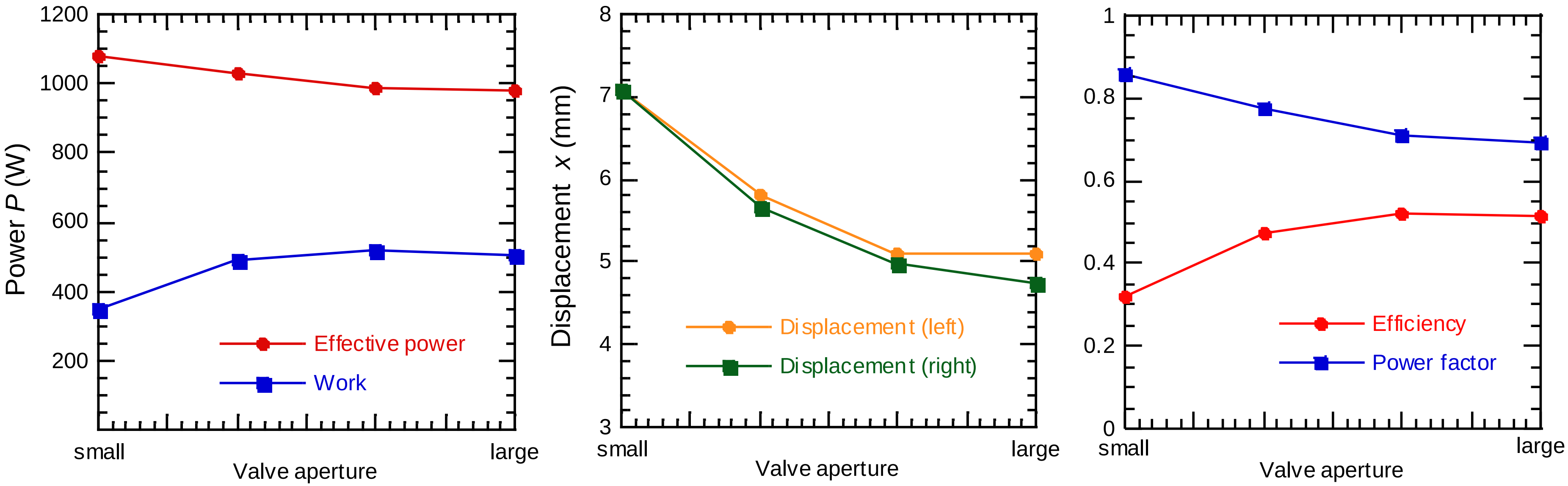

(a) Input power and *PV* work (b) Displacement (c) Efficiency and power factor

Fig.15 Experimental results under load condition

Next target:
- Improvement of efficiency
- Test at the rated displacement
- Comparison of analysis results

京都大学 KYOTO UNIVERSITY

5. Development and test of the pulse-tube cryocooler

Cooling test of the pulse-tube cryocooler coupled with the compressor

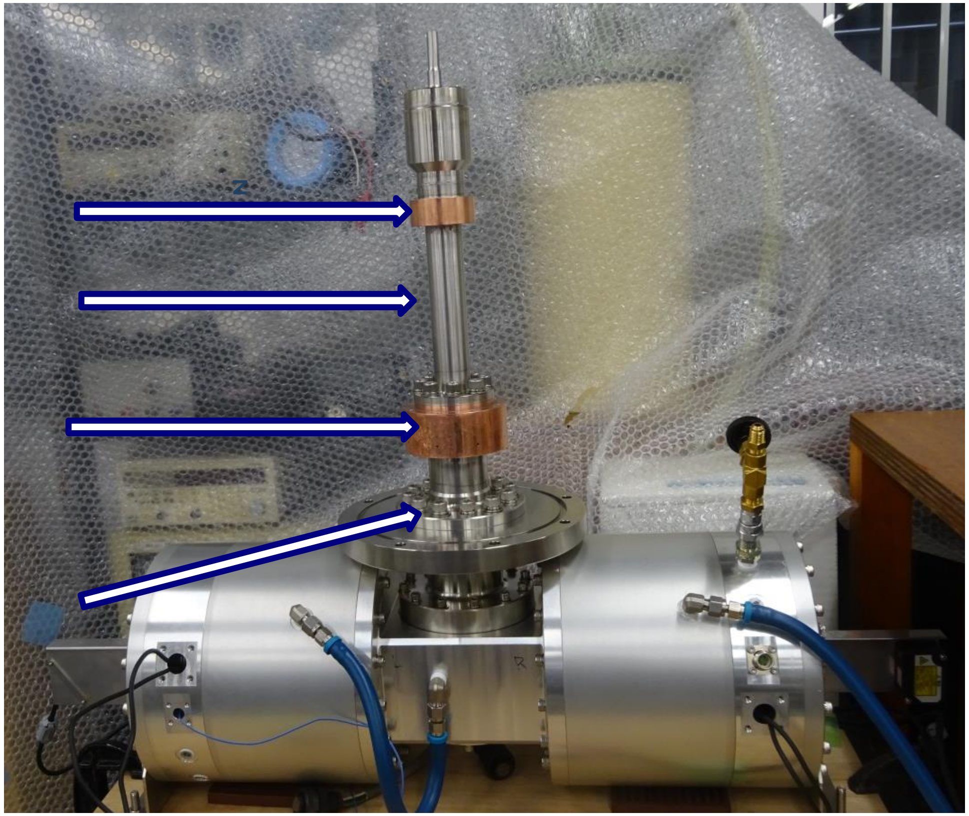

Fig.16 Photograph of pulse-tube cryocooler

Evaluation of pulse-tube cryocooler at 77 K

Table2 Specifications of buffer unit

Buffer tank volume	3485 cm^3 (1 gal)
Copper pipe length	2 m

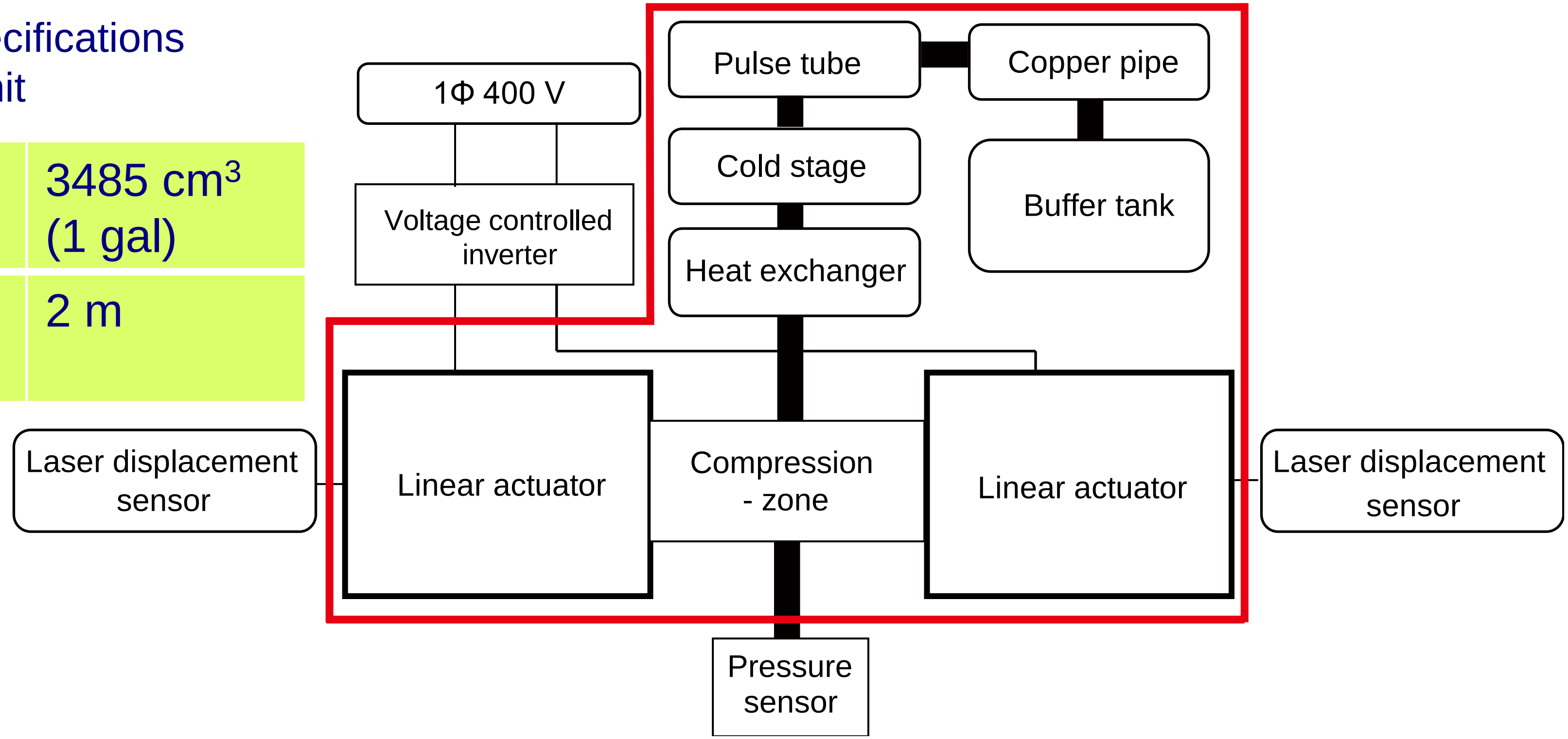

Fig.17 Schematic diagram of experiment of pulse-tube cryocooler

5. Development and test of the pulse-tube cryocooler

Pressure 2.5 MPa, Input 160 V, Operational temperature 77 K

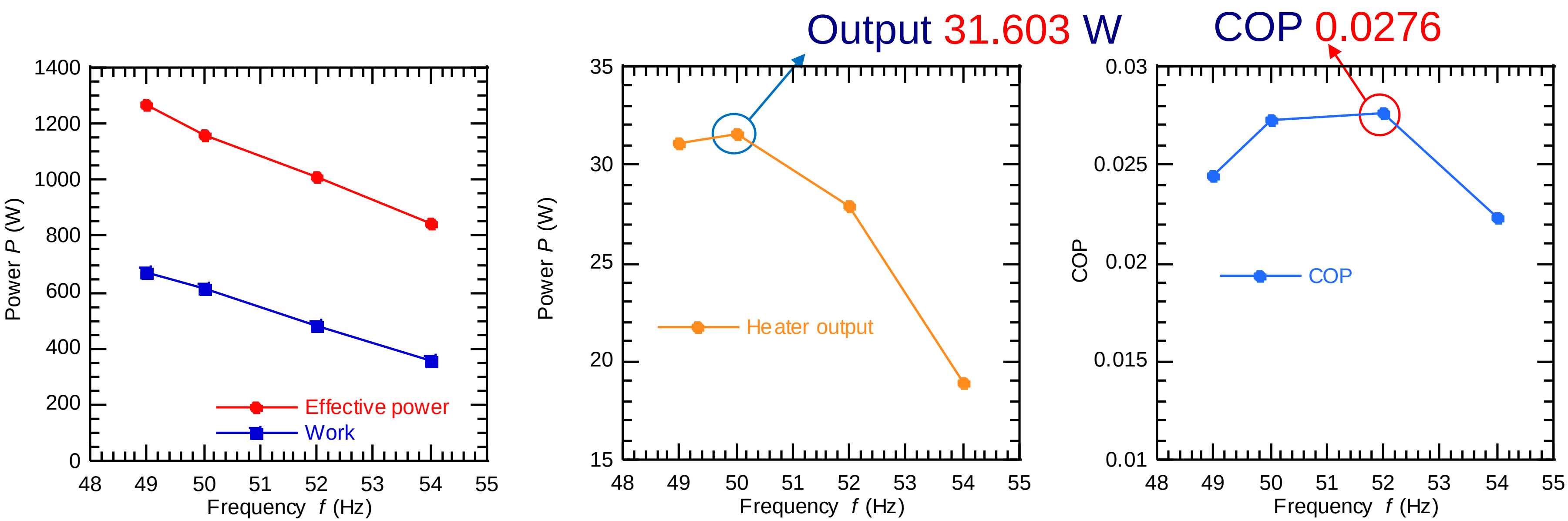

(a) Input power and *PV* work (b) Cryocooler output (c) COP

Fig.18 Experimental results of pulse-tube cryocooler

Next target: Re-try of cooling test with the improved compressor

6. Conclusion

・ Development of linear actuator-type compressor for cryocooler

・ Modeling the linear actuator by the use of electromagnetic field analysis code coupled with kinetic equation

・ Agreement between experimental and analytical results by considering the nonlinear B-H curve of the iron core

・ Obtaining analytical results which show possibility of high efficiency as well as high power factor

・ Conducting cooling test of the pulse-tube cryocooler

6. Conclusion

Future plan

・Experiment at the rated displacement and development of analysis code considering thermodynamics of He gas

・Development of Stirling-type cryocooler for HTS-ISM system